BES Analysis Memo

Partial Wave Analysis of $J/\Psi \to \gamma K^+K^-$ and $\gamma\pi^+\pi^-$

BES Collaboration [a], D.V. Bugg [b]

[a] *Institute of High Energy Physics, Beijing 100039, P. R. China*

[b] *Queen Mary, London E1 4NS, UK*

January 26, 2001

Abstract

New data from BES are presented on J/Ψ radiative decays to K^+K^- and $\pi^+\pi^-$, from a sample of 24M J/Ψ hadronic interactions in the BES II detector. In the $\gamma(K\bar{K})$ final state, $f_2'(1525)$ and $f_0(1710)$ are conspicuous; the latter peaks at a mass of 1735 MeV with a width of 180 ± 20 MeV, both slightly above earlier observations of $f_0(1710)$. In $\gamma(\pi\pi)$, a strong $f_2(1270)$ is observed and a smaller $J^{PC} = 0^{++}$ signal at ~ 1750 MeV. The dominance of $f_0(1710) \to K\bar{K}$ over decays to $\pi\pi$ in present data contrasts strongly with data on $J/\Psi \to \phi\pi^+\pi^-$ and ϕK^+K^-, where a $\pi\pi$ signal is observed at 1770 MeV but without any corresponding signal in $K\bar{K}$. The four sets of data taken together demand the presence of two 0^+ states, (i) $f_0(1710)$ decaying dominantly to $K\bar{K}$ and (ii) $f_0(1770)$ decaying dominantly to $\pi\pi$ and 4π. If the $\pi\pi$ signal is interpreted as coming from $f_0(1770)$, the branching ratio $f_0(1770) \to 2\pi/f_0(1770) \to 4\pi = (9.6 \pm 3.6)\%$. The $\gamma(\pi\pi)$ data also require interfering contributions from $f_0(1500)$ and the broad $f_0(400-1200)$. The $f_0(400-1200)$ also makes a small but definite contribution to $\gamma(K\bar{K})$.

Introduction

Quantum Chromodynamics(QCD) admits the possibility of colorless bound states of two or more gluons which have been named glueballs. Radiative decays of the J/Ψ have been suggested [1] as promising modes for glueball searches. The ratio of J/Ψ decays via γgg to those via ggg, according to perturbative QCD, is

$$\frac{\Gamma(J/\Psi \rightarrow \gamma gg)}{\Gamma(J/\Psi \rightarrow ggg)} = \frac{36}{5} e_q^2 \frac{\alpha}{\alpha_s} [1 + \frac{2.2\alpha_s}{\pi} + \cdots]^2$$

For $\alpha_s = 0.2$, this leads to a branching fraction BR$(J/\Psi \rightarrow \gamma 2g) \sim 5 - 10\%$. Thus, a substantial fraction of all J/Ψ decays are expected to be produced through the radiative decay diagram. Hadronic final states produced from the two gluon system have C = + and I = 0.

It has been calculated [2] that $J^{PC} = 0^{++}, 0^{-+}, 2^{++}$ dominate the $J/\Psi \rightarrow \gamma X$ final state and that $J^{PC} = 1^{--}$ and 1^{-+} are suppressed. The final states most accessible are those containing two or three pseudoscalars. Two pseudoscalars can combine to produce states with $J^{PC} = 0^{++}, 2^{++}$, while three pseudoscalars can form $J^{PC} = 0^{-+}$ states.

Many different QCD-based models and calculations make predictions for such states: bag, models, constituent-glue models, flux-tube models, QCD sum rules and lattice gauge theory. Recent lattice QCD calculations are converging towards agreement and we expected that the lattice results will be the most relevant, since they originate from QCD. The lightest glueball is found to be a 0^{++} state with the following masses from the different lattice calculations: 1550±50 MeV [3], 1600±160 MeV [4], 1648±58 MeV [5], and 1730±100 MeV [6]. The difference between these results lies mainly in how the mass scale is set, and mixings with $q\bar{q}$ and $q\bar{q}q\bar{q}$ states could modify these predictions.

The $f_0(1500)$ has been touted as a likely candidate for a "glueball". The evidence is circumstantial: it is produced primarily in glue-rich eviroments; its mass and width are consistent with theoretical prediction; and it overpopulates the $q\bar{q}$ states if in this mass region we assume it is not the $s\bar{s}$ state. Direct evidence, however, is lacking. Most of the data on the $f_0(1500)$ are from the Crystal Barrel Collaboration, who resolved two scalar states in this mass region [7] and who determined its decay branches to a number of final states, including $\pi^0\pi^0, \eta\eta, \eta\eta', K_L K_L$ and $4\pi^0$, all using $\bar{p}p$ annihilation at rest in liquid hydrogen. The $f_0(1500)$ has also been observed by the OBELIX experiment [8] in the $\bar{n}p \rightarrow \pi^+\pi^+\pi^-$ reaction for neutrons in flight, by the WA91 [9] and WA102 [10] Collaborations, in "gluerich" central production reactions $pp \rightarrow p_f(\pi^+\pi^-\pi^+\pi^-)p_s$ and $pp \rightarrow p_f(\pi^+\pi^-)p_s$, and most recently in Fermilab experiment E690 [11]. There is evidence of $J/\Psi \rightarrow \gamma f_0(1500)$ with $f_0(1500) \rightarrow \pi^+\pi^-\pi^+\pi^-$ [12] [13] and perhaps also with $f_0(1500) \rightarrow \pi^+\pi^-$ [14], but S-wave structure in the K^+K^- and K_SK_S final states seems absent in this mass region for J/Ψ radiative decay.

The $f_0(1710)$ is the main competitor of the $f_0(1500)$ for status as the lightest glueball. In fact, the IBM group compares the measured properties of the $f_0(1710)$ to their calculations and directly argue that it must be the lightest scalar glueball [15]; since the $f_0(1710)$ was first discovered by the Crystal Ball Collaboration in $J/\Psi \to \gamma\eta\eta$ [16], there has been considerable interests in its experimental and theoretical studies. The $f_0(1710)$ displays clear glueball characteristic in that it is produced in glue-rich production mechanisms and is either not seen or is heavily suppressed in normal hadronic interactions. In addition, the $f_0(1710)$ is observed to decay dominantly to $K\bar{K}$ and yet it is not observed in K^-p interactions [17]. However, the spin of the $f_0(1710)$ has been uncertain with $J = 0$ or 2 being possible, and it was called as "$f_J(1710)$" for a long period. Tab. 1 shows the experimental results of the $f_0(1710)$ study in chronological order.

At the beginning, the results were very controversial, and the $f_0(1710)$ was allocated spin two by many experiments [18] [19]. With the improvement of statistics as well as spin-parity analysis method, during 1990s, especially in recent years, the spin analysis of the $f_0(1710)$ has been performed may times through different processes [14] [12] [20] [21] [22] [13]. From the results shown in Tab. 1, such an interesting and important tendency could be found: nearly all the analyses reached the same conclusion that spin zero is preferred over two whereas no reports of 2^{++} are given. The Particle Data Group 2000 assigns the $f_0(1710)$ to be spin zero [23].

In the mass range 1700-1800 MeV, another 0^{++} state is also to be expected, a non-strange radial excitation of the $f_0(1370)$ [24]. Both are likely to mix with the glueball anticipated in this mass range, so their appearance in J/Ψ radiative decays is not surprising. The radial excitation is naturally interpreted as $f_0(1770)$, because of its appearance in $\pi\pi$ and 4π. In a study of $J/\Psi \to \phi(K\bar{K})$ and $\phi(\pi\pi)$, we likewise observe 0^+ signals in $K\bar{K}$ and $\pi\pi$ which are distinct in mass from PDG values of $f_0(1710)$ [25].

The processes $J/\Psi \to \gamma K^+K^-$ and $\gamma\pi^+\pi^-$ have been previously studied in the Mark III [18] [14] and DM2 [26] [27] experiments. However, from recent experimental results their analyses are questionable and not complete. At that time, the $f_0(1500)$, $f_0(1710)$ and $f_0(1370)$ were still not established, and not adopted naturally. Here we present new data taken in 1999-2000 on $J/\Psi \to \gamma K^+K^-$ and $\gamma\pi^+\pi^-$ with significantly larger statistics; the present sample is from 24M J/Ψ hadronic interactions in the upgraded BES detector. This upgrade includes a new main drift chamber (MDC) and improved time-of-flight scintillators. The intensity of the BEPC accelerator has been increased to an average luminosity of 4.0×10^{30} $cm^{-1}s^{-1}$. As mentioned before, J/Ψ radiative decay

Process	Collaboration	M(MeV)	Γ(MeV)	J^{PC}
$J/\Psi \to \gamma\eta\eta$	C. B.(82)	1640 ± 50	200^{+100}_{-70}	2^{++}
$\pi^- p \to K^0_s K^0_s n$	BNL(82)	1771^{+77}_{-53}	200^{+156}_{-9}	0^{++}
$\pi^- N \to K^0_s K^0_s n$	FNAL(84)	1742 ± 15	57 ± 38	——
$\pi^- p \to \eta\eta N$	GAMS(86)	1755 ± 8	< 50	0^{++}
$J/\Psi \to \gamma K^+ K^-$	MARKIII(87)	1720 ± 14	130 ± 20	2^{++}
$J/\Psi \to \gamma K^+ K^-$	DM2(88)	1707 ± 10	166 ± 33	——
$pp \to p(K\bar{K})p$	WA76(89)	1713 ± 10	181 ± 30	2^{++}
$J/\Psi \to \gamma K\bar{K}$	MARKIII(91)	1710 ± 20	186 ± 30	0^{++}
$p\bar{p} \to \pi^0\eta\eta$	E760(93)	1748 ± 10	264 ± 25	$(even)^{++}$
$J/\Psi \to \gamma 4\pi$	MARKIII data	1750 ± 15	160 ± 40	0^{++}
	D. Bugg(95)			
$J/\Psi \to \gamma K^+ K^-$	BES(96)	$1696 \pm 5^{+9}_{-34}$	$103 \pm 18^{+30}_{-11}$	2^{++}
		$1781 \pm 8^{+10}_{-31}$	$85 \pm 24^{+22}_{-19}$	0^{++}
$J/\Psi \to \gamma K\bar{K}$	MARKIII data	1704^{+16}_{-23}	124^{+52}_{-44}	0^{++}
	W. Dunwoodie(97)			
$pp \to p(K\bar{K})p$	WA102(99)	1730 ± 15	100 ± 25	0^{++}
$pp \to p(\pi^+\pi^-)p$	WA102(99)	1750 ± 25	105 ± 34	0^{++}
$pp \to p(\pi^+\pi^-)p$	WA76(99)	1710 ± 20	160 ± 30	0^{++}
$J/\Psi \to \gamma 4\pi$	BES(2000)	1740^{+20}_{-25}	135^{+40}_{-25}	0^{++}

Table 1
The experimental results of the $f_0(1710)$ study in chronological order.

is a glue-rich mechanism, and comparision with other experiments such as central production is cleaner. Therefore $J/\Psi \to \gamma K^+K^-$ and $\gamma\pi^+\pi^-$ provide an ideal experimental field to study the properties of the $f_0(1500)$, $f_0(1710)$, $f_0(1370)$ and other meaningful questions by using the new BES J/Ψ data.

The $\gamma\pi^+\pi^-$ channel is the largest and best studied of the radiative decays to two pseudoscalars. Unfortunately, the $\gamma\pi^+\pi^-$ channel is also the one most affected by backgrounds, primarily because of feed-down from the very large $J/\Psi \to \rho\pi \to \pi^+\pi^-\pi^0$ decay mode. Both the event selection and background problems for the $J/\Psi \to \gamma K^+K^-$ channel are quite similar to the $\gamma\pi^+\pi^-$ case. The major differences are the need to employ particle identification criteria and the presence of non vector-pseudoscalar $K^+K^-\pi^0$ backgrounds. In the following part, We describe the cuts for these two channels; the difference between them will be pointed out especially.

Event Selection

An initial selection of two-prong charge-zero events with at least one neutral track is performed. The charged particles are each required (i) to have good helix fits with complete error matrices so that kinematic fitting can be performed, (ii) to deposit less than 1.0 GeV in the shower counters to suppress radiative Bhabhas, and (iii) not to register hits in the muons counters so that obvious $\gamma\mu^+\mu^-$ events are removed. Further radiative di-lepton suppression is accomplished by requring that the tracks be acollinear by at least $5°$.

Particle Identification

For the γK^+K^- channel, in order to reduce the background from final states with pions and electrons each event is required to have at least one track which satisfies $W_K > W_\pi$, $W_K > W_e$, where W_K, W_π, W_e are the TOF weights of K, π and electron respectively. In addition, when the momentum of the charged track lower than 0.6 GeV/c, requring that $W_K > W_\pi$, $W_K > W_e$. Although π - K separation by BES II TOF may be ambiguous for a single high momentum track, the ability of the TOF system to separate kaons from pions at momenta below 0.6 GeV/c is satisfactory. We do not impose two TOF measurements for the following reasons:

- In the $f_2'(1525) - f_0(1710)$ region, where the π background is small, it does not improve the signal to background ratio.

- It has a drawback on efficiencies, especially for the $f_2'(1525)$ where one of the kaons is likely to be slow enough not to reach the TOF counter before its decay.

Particle identification applied in the $\gamma\pi^+\pi^-$ channel is much looser than in γK^+K^-; the charged track with momentum lower than 0.6 GeV should be identified by TOF as a pion, because the π particle fraction equals to 87.5 ± 1.3 % in J/Ψ decay [28] while here the momenta of the charged tracks are too high to be distinguished; this allows us to keep relatively high efficiency and low kaon or proton efficiency as well.

Photon Criteria

We require at least one neutral track satisfying the following criteria. More than one photon per event is allowed due to the fake photons which come from the interactions of charged tracks in the shower counter.

(i) Hit in Barrel Shower Counter (BSC)
(ii) Layers > 1 or $Esc > 100$ MeV, and shower starts before layer 6
(iii) Angle between the cluster entering and going through BSC should be less than $30°$

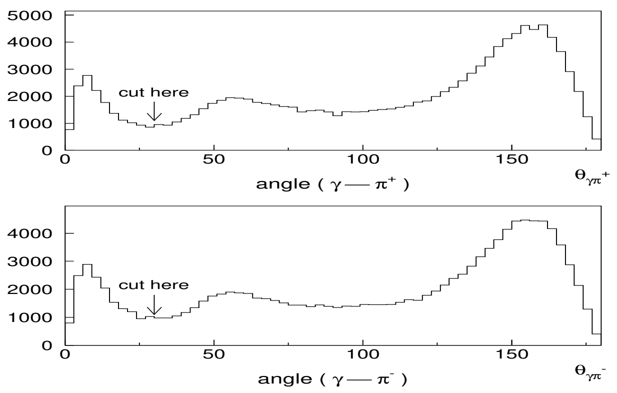

Fig. 1. Angle between photon and each charged pion (data).

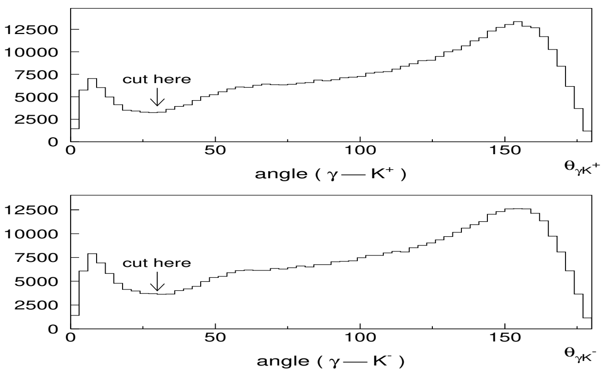

Fig. 2. Angle between photon and each charged kaon (data).

(iv) Angle between photon and each charged track is required to be larger than $30°$; Fig. 1 and 2 show the distributions of this angle.

One next requires the two charged tracks and the good photon in the event to be kinematically consistent with a radiative decay. This is performed in two stages. One first cuts on the measured quantities:

$|U| = |(E_{miss} - |\vec{P}_{miss}|)| < 0.15$ GeV

$P^2_{t\gamma} = 4|\vec{P}_{miss}|^2 sin^2\frac{\theta_\gamma}{2} < 0.002$ GeV^2

$(\alpha_{\pi^0})_{min} > 8°$ when the number of photons $N_\gamma \geq 2$;

U and $P^2_{t\gamma}$ [29] are two conventional and important quantities in J/Ψ radiative decays, where E_{miss} and $\vec{P}_{miss}$ are the missing energy and momentum calculated using the better-measured charged particle momenta, and θ_{miss} is the angle between the missing momentum vector and the photon shower. Especially, U, whose distribution is gaussian (cf., Fig. 3 and 4), is a linear variable of E_{miss} and nearly independent of $\pi\pi$ or KK invariant masses. $|U| < 0.15$ GeV is just corresponding to $\sim 2.5\sigma$ in the resolution. $P^2_{t\gamma}$ measures the agreement between the missing momentum recoiling against the charged tracks and the angles of the photon in the event. The π^0 background is approximately flat in this quantity for values up to $P_{t\gamma}^2 \sim m_{\pi^0}^2$, whereas the radiative signal is peaked at small values $P_{t\gamma}^2 \simeq 0.001$ GeV^2. The distributions in $P_{t\gamma}^2$ for the $\gamma\pi^+\pi^-$ and γK^+K^- events are shown in Fig. 5 and 6. Signal events are required to have $P_{t\gamma}^2 < 0.002$ GeV^2; this cut suppresses about 50% of the π^0 background.

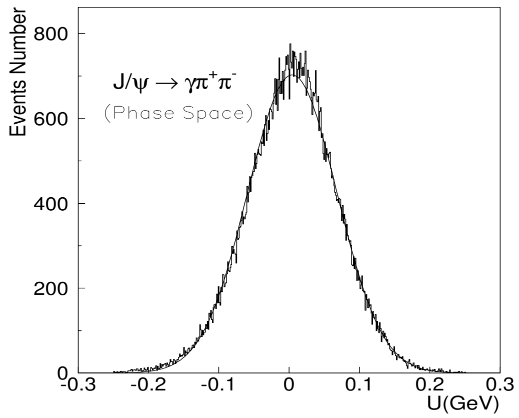

Fig. 3. The U distribution of the Monte Carlo events for $J/\Psi \to \gamma\pi^+\pi^-$.

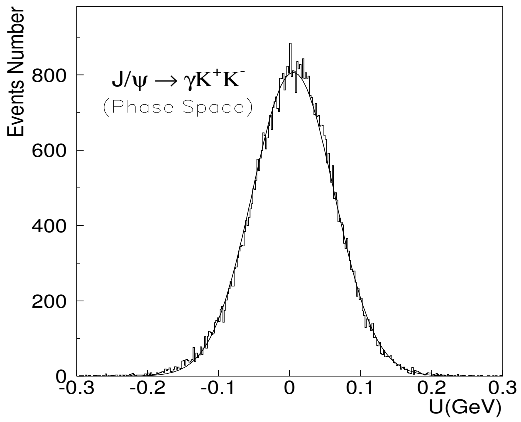

Fig. 4. The U distribution of the Monte Carlo events for $J/\Psi \to \gamma K^+K^-$.

When the number of photons $N_\gamma \geq 2$, the events with π^0 are removed by using the quanlitity α_{π^0} angle [30]. The multiphoton events having $(\alpha_{\pi^0})_{min} < 8°$ are discarded, where $(\alpha_{\pi^0})_{min}$ is the minimum value of all possible combinations of photon pairs. The advantage of α_{π^0} is that it is independent of the measurement of photon energy. The distributions in $(\alpha_{\pi^0})_{min}$ for the $\gamma\pi^+\pi^-$ and γK^+K^- events are shown in Fig. 7 and 8.

Further reduction of π^0 and di-lepton backgrounds are next made.

The two body decay behavior of $\rho - \pi$ decay of J/Ψ is used to remove $J/\Psi \to \rho\pi$ events in the $\gamma\pi^+\pi^-$ channel: Events having one charged pion momentum in the region $|P_{\pi^\pm} - 1450| < 40$ MeV and the invariant mass of the other charged pion and π^0 in the ρ mass region $|M_{\pi^\mp\pi^0} - M_{\rho^\mp}| < 75$ MeV are removed. When

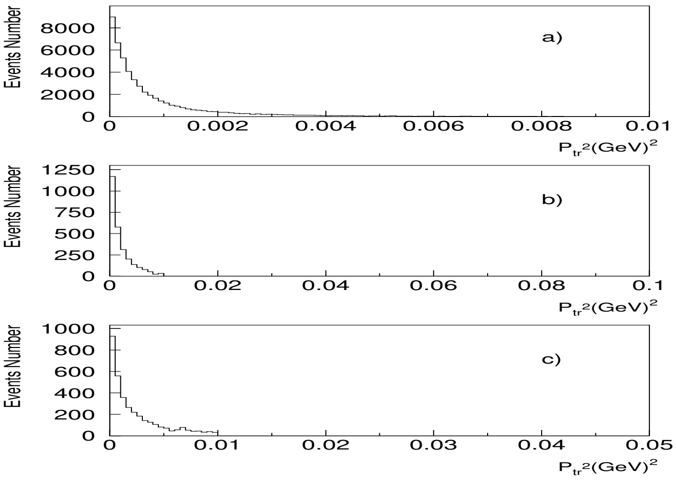

Fig. 5. $P_{t\gamma}^2$ distributions a) $J/\Psi \to \gamma\pi^+\pi^-$ (Monte Carlo); b) $J/\Psi \to \rho\pi$ (Monte Carlo); c) $J/\Psi \to \gamma\pi^+\pi^-$ data sample.

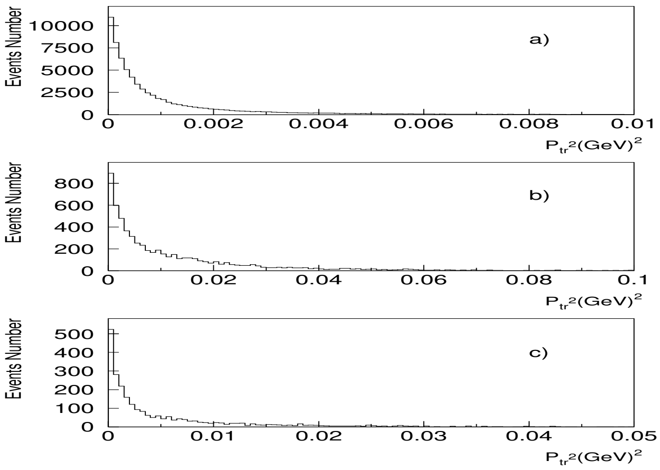

Fig. 6. $P_{t\gamma}^2$ distributions a) $J/\Psi \to \gamma K^+K^-$ (Monte Carlo); b) $J/\Psi \to K^{*\pm}K^{\mp}$ (Monte Carlo); c) $J/\Psi \to \gamma K^+K^-$ data sample.

$M_{\pi^\mp\pi^0}$ is calculated, the momentum of the π^0 is obtained from $P_{\pi^0} = P_{miss}$. And the two body decay $J/\Psi \to K^{*\pm}K^{\mp}$ is rejected heavily by using the analogous method in the γK^+K^- channel. The di-lepton contamination for $\gamma\pi^+\pi^-$ channel is more than the γK^+K^- one because of the lower mass of the pion. Therefore we use more strict cuts in the $\gamma\pi^+\pi^-$ channel to remove the di-lepton backgrounds. For $\pi\pi$, we require: (a) the energy deposit in BSC of each track $E_{SC} < 600$ MeV, and (b) the angle between each track and the positron beam direction satisfies $|cos\theta| < 0.75$. While for KK, we require: (a) $E_{SC} < 1.0$ GeV and (b) if the momentum of charged track is greater than 600 MeV, $E_{SC}/P < 0.8$; $|cos\theta| < 0.84$.

Finally, events are 4-C kinematically fitted to obtained better mass resolution and to suppress backgrounds further by the requiremets:

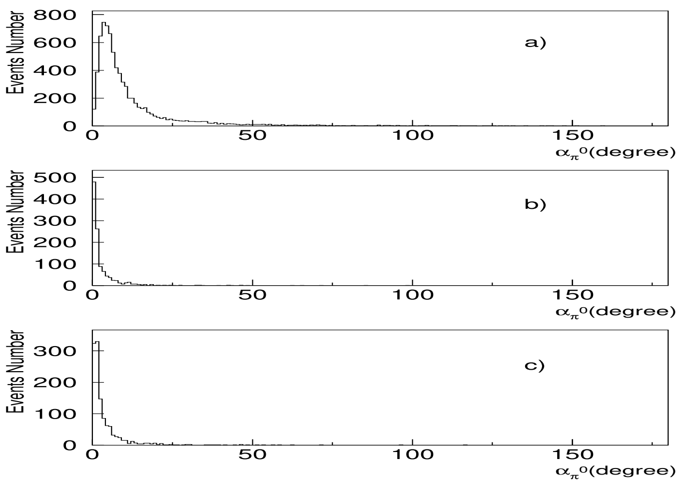

Fig. 7. $(\alpha_{\pi^0})_{min}$ distributions a) $J/\Psi \to \gamma\pi^+\pi^-$ (Monte Carlo); b) $J/\Psi \to \rho\pi$ (Monte Carlo); c) $J/\Psi \to \gamma\pi^+\pi^-$ data sample.

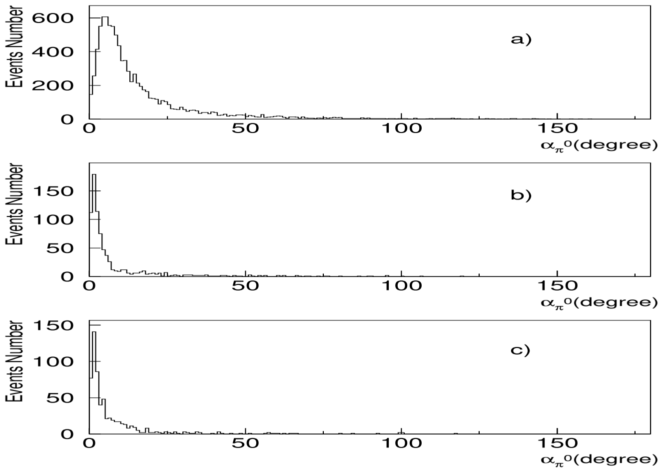

Fig. 8. $(\alpha_{\pi^0})_{min}$ distributions a) $J/\Psi \to \gamma K^+K^-$ (Monte Carlo); b) $J/\Psi \to K^{*\pm}K^{\mp}$ (Monte Carlo); c) $J/\Psi \to \gamma K^+K^-$ data sample .

$$\chi^2_{\gamma\pi^+\pi^-} < 20,\ \ \chi^2_{\gamma K^+K^-} > 10,\quad \chi^2_{\gamma\pi^+\pi^-} < \chi^2_{\gamma K^+K^-}\quad (\gamma\pi^+\pi^-\text{ channel})$$
$$\chi^2_{\gamma K^+K^-} < 20,\ \ \chi^2_{\gamma\pi^+\pi^-} > 10,\quad \chi^2_{\gamma K^+K^-} < \chi^2_{\gamma\pi^+\pi^-}\quad (\gamma K^+K^-\text{ channel})$$

The $\pi^+\pi^-$ mass spectrum after all these cuts is shown in Fig. 9. The shaded region is an absolute prediction of the $\rho\pi$ background contribution which is based on a Monte Carlo simulation, and the measured $\rho\pi$ branching ratio fraction for the normalization. The background shape seems to be quite reasonable, indicating that the di-lepton contamination and other background sources are under control.

One notes six prominent features:

1. There is a large peak at the ρ^0 mass corresponding to feed-through from $J/\Psi \to \rho^0\pi^0$.

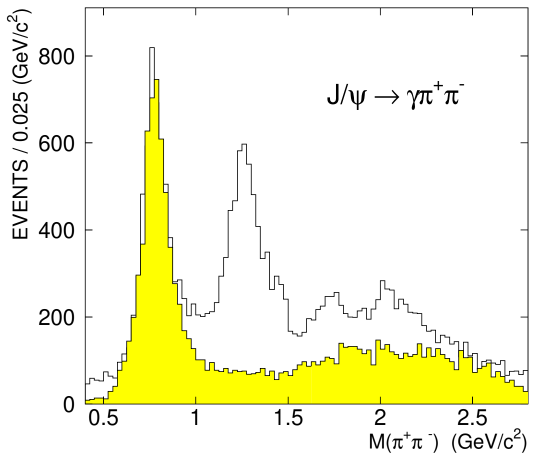

Fig. 9. $\pi^+\pi^-$ mass spectrum after final cuts.

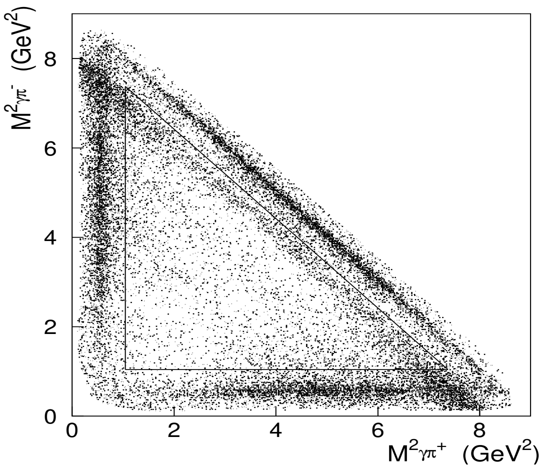

Fig. 10. $\gamma\pi^+\pi^-$ Dalitz plot.

2. The very low-mass part of the $\pi^+\pi^-$ spectrum is not well described by the $\rho\pi$ background.

3. A very large $f_2(1270)$ signal is evident.

4. The $f_2(1270)$ line shape is very asymmetric. A sharp dip, characteristic interference phenomena, is apparent at $m_{\pi^+\pi^-} \sim 1.5$ GeV$/c^2$.

5. An enhancement at $m_{\pi^+\pi^-} \sim 1.75$ GeV$/c^2$ is visible.

6. A final bump at $m_{\pi^+\pi^-} \sim 2.1$ GeV$/c^2$ is clearly present over the $\rho\pi$ background.

Fig. 10 shows the Dalitz plot for the $\gamma\pi^+\pi^-$ final state. The $\rho^\pm\pi^\mp$ states are visible as bands parallel to the axes of the plot. The $\pi^+\pi^-$ states appear as diagonal bands.

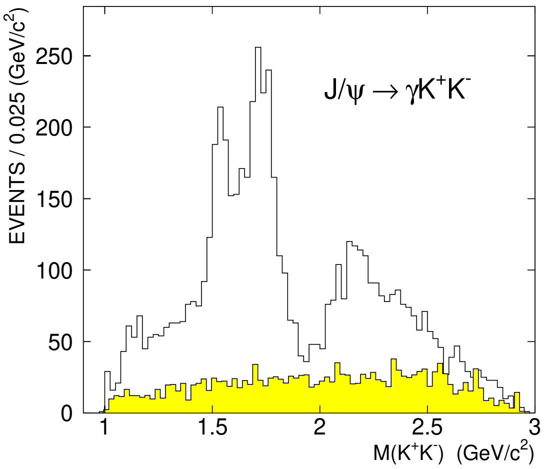

Fig. 11. K^+K^- mass spectrum after final cuts.

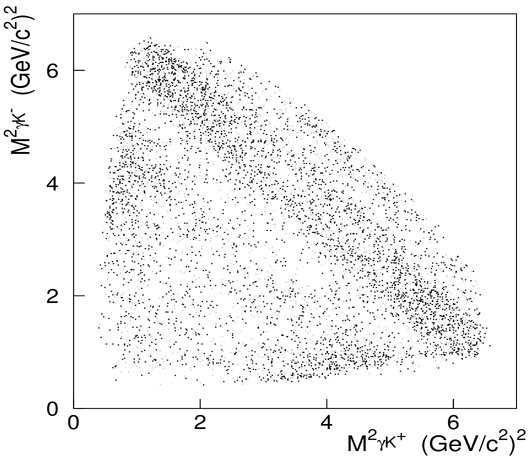

Fig. 12. γK^+K^- Dalitz plot.

Fig. 11 shows the K^+K^- mass spectrum after final cuts, and Fig. 12 the Dalitz plot. The resonant structures in the mass regions of the $f_2'(1525)$ and the $f_0(1710)$ are very clearly visible in both figures and a bump at $m_{K^+K^-} \sim$ 2.1 GeV is present over the background. In Fig. 12, Vertical and horizontal bands along the axes are due to the K^*K and $\rho\pi$ backgrounds. The genuine radiative events form diagonal bands. The shaded region in Fig. 11 indicates the estimated backgrounds which will be studied in the following part.

Detection Efficiency

The detection efficiencies, averaged over a phase space production model, are shown in Fig. 13 and 14 respectively. They have a slight dependance on the invariant masses: almost constant up to 2 GeV/c^2 and then decreasing smoothly to 2.9 GeV/c^2. The fall-off at high mass is a consequence of the acollinearity cut.

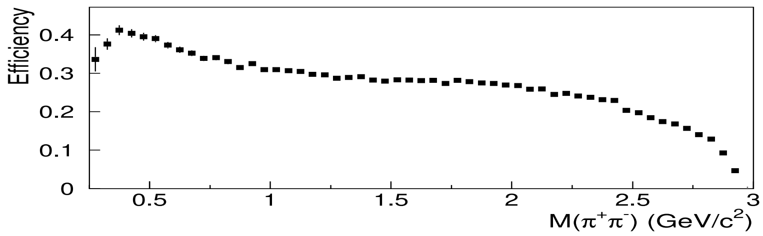

Fig. 13. Mean $\pi^+\pi^-$ detection efficiency vs. $\pi^+\pi^-$ mass.

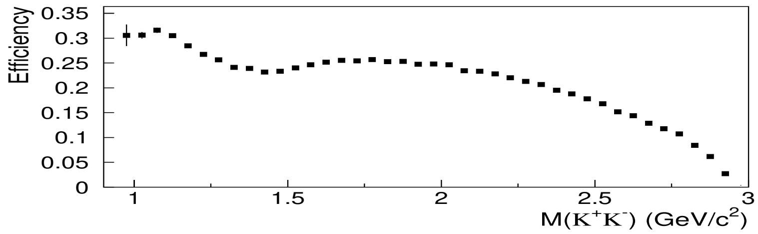

Fig. 14. Mean K^+K^- detection efficiency vs. K^+K^- mass.

The outer radius of the MDC (1.15 m) is comparable to the proper decay length of a kaon (3.7m); kaons produced in J/Ψ decays often decay within the BES detector. The minimum and maximum kaon momenta for different K^+K^- masses, are displayed in Fig. 15. The vanishing minimum momentum that occurs at $m_{K^+K^-} \sim 1.35$ GeV is the result of a kinematic cross-over which takes place when the velocity of the K^+K^- system is equal to the velocity of the kaons in the K^+K^- center of mass. This kinematic effect combines with the kaon detection efficiency not only to produce a reduction in the overall efficiency in the 1.4 GeV mass region but also is reflected in the efficiency function of the polar angle of the positive kaon in the K^+K^- center of mass. This is significant for the $f_2'(1525)$ branching ratio measurement and spin analysis.

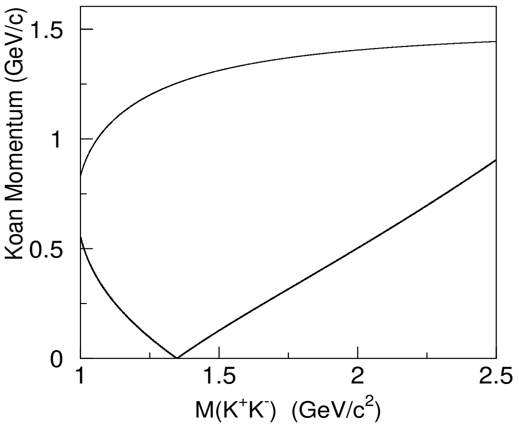

Fig. 15. Variations of K meson's maximum and minimum momenta with $m_{K^+K^-}$ and the upper line corresponding to maximum, the lower line corresponding to minimum.

Background Study

$\gamma\pi^+\pi^-$ channel

$\rho\pi$ production with asymmetric decay is by far the dominant source of background in this channel. The $\gamma\pi^+\pi^-$ data sample is contaminated heavily, especially in the high mass region by $\rho^\pm\pi^\mp$. Di-lepton backgrounds which are peaked at $\pi^+\pi^-$ masses are estimated to be nearly zero from the Monte Carlo simulation using the above cuts. $K^+K^-\pi^0$ background is quite similar to $\rho\pi$ expect that there is no $\phi\pi^0$ component analagous to $\rho^0\pi^0$. The π - K mass difference provides kinematical separation except for high momentum tracks. The Monte Carlo yields an efficiency of 1.6×10^{-3} for reconstructing K^*K as $\gamma\pi^+\pi^-$. Using the branching ratio for $J/\Psi \to K^*K$ and including the proper Clebsch-Gordon coefficients, one estimates a background of ~ 48 events. This background peaks at $m_{\pi^+\pi^-} \sim 2.4$ GeV/c^2, and is totally negligible for $\pi^+\pi^-$ masses below 2 GeV/c^2. Misidentification of the two kaon radiative decays as two-pion decays is potentially very serious since the K^+K^- spectrum is dominated by two resonances: $f_2'(1525)$, and $f_0(1710)$. The misidentification probability for events coming from these states is estimated through the Monte Carlo to be 1.96×10^{-3} and 2.72×10^{-3}, respectively. The two peaks feed in at $m_{\pi^+\pi^-} \sim 1.27$ and 1.57 GeV. These background contributions are dwarfed by that from $\rho\pi$.

γK^+K^- channel

- $\rho\pi$ background. The $\rho^0\pi^0$ events feed the K^+K^- mass region under 1.3 GeV/c^2, whereas $\rho^\pm\pi^\mp$ events are mostly over 2 GeV/c^2.

- $K^+K^-\pi^0$ background, which consists of two pieces. One is the two body decay behavior of K^*K which contaminates mainly the 2 to 3 GeV/c^2 region; the other is the non-resonant $K^+K^-\pi^0$ background events which feed the K^+K^- mass region uniformly. And $\mathcal{B}(J/\Psi \to K^+K^-\pi^0)_{non-K^*K} = (4.7 \pm 1.2 \pm 1.3) \times 10^{-4}$ [31].

- $\gamma K^+K^-\pi^0$ events from $\gamma\eta(1440)$ which feed the K^+K^- mass region around 1.1 GeV/c^2. Although the branching ratio of this sub-process is relatively small, the surviving events comprise the main background in the low K^+K^- mass region.

- $\gamma\pi^+\pi^-$ events mainly from $J/\Psi \to \gamma f_2(1270) \to \gamma\pi^+\pi^-$ which peak at $\sim 1.5-1.6$ GeV/c^2. To reduce such background contributions and any residual radiative dilepton events, the charged tracks are subject to particle identification requirements based on TOF information.

- Radiative Bhabha and Dimuon events which are peaked at high K^+K^- masses.

- Unknown multiphoton events such as $J/\Psi \to K^+K^- + neutrals \to (n\gamma)K^+K^-$, $J/\Psi \to \pi^+\pi^- + neutrals \to (n\gamma)\pi^+\pi^-$ are rejected by using U cut, particle identification and kinematic fit effectively.

The Monte Carlo simulations of the detection efficiencies as well as the estimated events of the main background channels included in data samples for $\gamma\pi^+\pi^-$ and γK^+K^- are summarized in Tab. 2.

ε (detection efficiency)	$J/\Psi \to \gamma\pi^+\pi^-$		$J/\Psi \to \gamma K^+K^-$	
$\gamma\pi^+\pi^-$	29.58%			
γK^+K^-			23.71%	
$\rho^\pm\pi^\mp$	2.87%	*5717*	6.8×10^{-4}	*142*
$\rho^0\pi^0$	5.98%	*6024*	2.0×10^{-5}	*2*
$K^{*\pm}K^\mp$	1.6×10^{-3}	*48*	2.25%	*676*
$K^+K^-\pi^0$	9.2×10^{-4}	*9*	4.35%	*435*
$\gamma f_2'(1525) \to \gamma K^+K^-$	1.96×10^{-3}	*1*		
$\gamma f_0(1710) \to \gamma K^+K^-$	2.72×10^{-3}	*3*		
$\gamma f_2(1270) \to \gamma\pi^+\pi^-$			1.4×10^{-4}	*3*
$\gamma\eta(1440) \to \gamma K^+K^-\pi^0$			4.8×10^{-4}	*1*

Table 2
Monte Carlo simulations of the detection efficiencies.

For the $\gamma\pi^+\pi^-$ data sample with 22970 events, $\rho\pi$ background is dominant, about 11523 events (50.2%). For γK^+K^- there are 6248 events; three background from K^*K, non-resonant $K^+K^-\pi^0$ and $\rho^\pm\pi^\mp$ are all important, totally about 1203 events (19.3%). Estimates of the $\pi^+\pi^-$ and K^+K^- mass spectra from these main backgrounds are shown in Fig. 9, 11.

Since resonances with spin higher than 2 are possible in the mass region over 2 GeV/c^2, a complete partial wave analysis would have to incorporate many spin and helicity states. However, the number of events in this region is small, but with high background; as a result, no reliable partial wave analysis can be carried out with the available statistics. Furthermore, for the $\gamma\pi^+\pi^-$ channel, there is a large ρ^0 signal at low $\pi^+\pi^-$ mass, and for the γK^+K^- channel, the backgrounds from $\gamma\eta(1440)$ and $\rho^0\pi^0$ contaminate the low mass range; a dip which may be caused by some interference exists around 1.95 GeV/c^2. Therfore, our study will cover only the mass range up to 1.95 GeV/c^2 and requires that $\mathrm{M}^2(\gamma\pi^\pm) > 1.1$ GeV^2 and $\mathrm{M}(\pi^+\pi^-) > 1.1$ GeV^2 (shown by the triangle in Fig. 10) while KK mass greater than 1.2 GeV in addition to avoid the uncertainty brought about by the background as well as to keep the consistency of the two parallel radiative decay channels. The present $\gamma\pi^+\pi^-$ data sample includes 4777 events with 803 background from $\rho\pi$ (16.8%); the γK^+K^- data sample includes 3605 events, and 198 (5.5%) from $\pi^0K^+K^-$, 77 (2.1%) from K^*K backgrounds.

Analysis Method

The maximum likelihood method is employed to fit the data. The probability density function $f(x_i;\alpha)$ with x_i as a set of independently measured quantities and α as a set of unknown parameters is given by:

$$f(x_i;\alpha) = \frac{d\sigma}{d\Phi}/\sigma,$$

where the total cross section $\sigma = \int \mid A_{total} \mid^2 d\Phi$ is calculated by using the Monte Carlo integration. The differential cross section is given by

$$\frac{d\sigma}{d\Phi} = \mid A^{0+} + A^{2+} + \cdots \mid^2 + BG,$$

here, BG is the background term, A^{0+}, A^{2+} are the amplitudes for scalar and tensor components respectively. In this paper the covariant tensor amplitude analysis is used to give the partial wave amplitudes.

A fit is made to the data in order to maximize the value of

$$\mathcal{L} = \prod_{i=1}^{N_{event}} f(x_i;\alpha).$$

Actually, $S = -ln\mathcal{L}$ is minimized in the fit.

In order to calculate the total cross section σ, 880,000 and 1,100,000 $J/\Psi \to \gamma\pi^+\pi^-$, γK^+K^- Monte Carlo events are generated respectively. Those events passing the data selection programs give the $\pi^+\pi^-$ phase space distribution shown in Fig. 16.

The technique employed in determing the background function is as follows. The background events obtained from Monte Carlo simulation using the corresponding $\rho\pi$, K^*K generators are included into the data sample, but with the opposite sign of log likelihood compared to data. These events cancel background within the data sample. A virtue of this technique is that it is not necessary to parametrise the form of the background as a function of masses or angles.

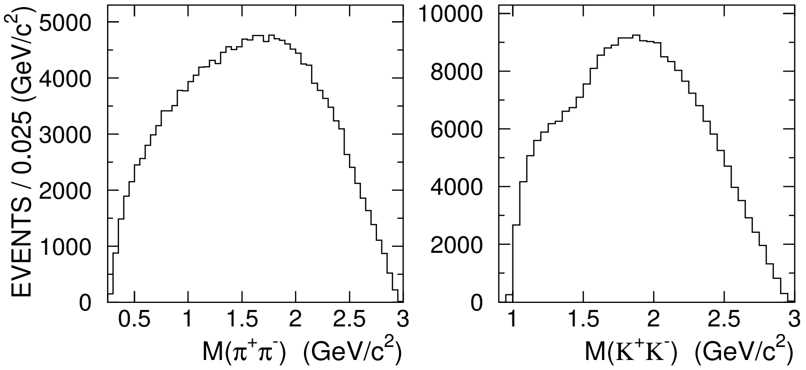

Fig. 16. Phase space distributions of $J/\Psi \to \gamma\pi^+\pi^-$ and $J/\Psi \to \gamma K^+K^-$.

Partial Wave Analysis

We begin by discussing the $\gamma(K^+K^-)$ data. Fig. 17 shows the K^+K^- invariant mass distribution. There are obvious peaks due to $f_2'(1525)$ and $f_0(1710)$. The detailed Monte Carlo simulation of the BES detector estimates a background of 275 events (7.6%). It is shown in Fig. 17 as B.G.

Partial waves have been fitted to the data for the following channels:

$$
\begin{aligned}
J/\psi &\to \gamma f_2'(1525) &(1)\\
&\to \gamma f_0(1710) &(2)\\
&\to \gamma f_0(400-1200) \equiv \sigma &(3)\\
&\to \gamma f_2(1270) &(4)\\
&\to \gamma f_0(1500). &(5)
\end{aligned}
$$

Of these, the first three are completely dominant. The minor contributions from $f_2(1270)$ and $f_0(1500)$ are introduced only for consistency with the fit to $\gamma(\pi^+\pi^-)$, using PDG values of branching ratios between $K\bar{K}$ and $\pi\pi$.

Amplitudes are fitted to relativistic tensor expressions [32]. For spin 0, E1 and E3 transitions from J/Ψ are allowed with $L = 0$ and 2 respectively. These two amplitudes differ only by a form factor, a function of the momentum k of the photon. For narrow resonances, this form factor has little effect, so there is effectively only one helicity amplitude; we therefore drop the $L = 2$ amplitude. For the broad $f_0(400-1200)$, the coupling constant may vary with mass and the $L = 0$ and $L = 2$ amplitudes may contribute with different mass dependence. Our procedure is therefore to fit the $L = 0$ amplitude with a coupling constant $\Lambda_1 + \Lambda_2 s$, where s is mass squared. For spin 2, there are three transitions: E1, M2 and E3. Since the transition is electromagnetic, the phases of the amplitudes (due to strong interactions in $\pi\pi$ and $K\bar{K}$ channels) are constrained to be the same; these phases are different for $\pi\pi$ and $K\bar{K}$ final states where strong interactions differ.

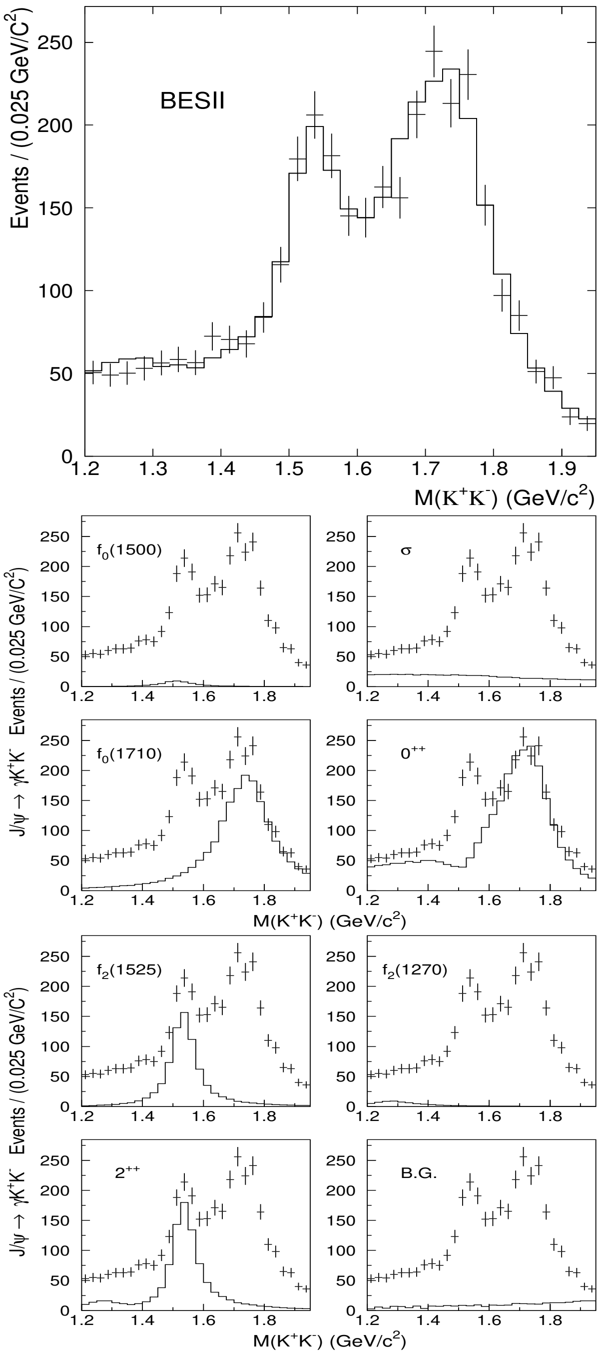

Fig. 17. The K^+K^- invariant mass distributions from $J/\psi \to \gamma(K^+K^-)$. The points are the data and the full histogram in the top panel shows the maximum likelihood fit. Histograms on subsequent panels show individual contributions from individual channels and the background (B.G.). The complete 0^+ and 2^+ contributions are also shown, including all interferences.

For $f_2'(1525)$ and $f_0(1500)$, we use PDG values [23] of masses and widths. A free fit to $f_2'(1525)$ gives a fitted mass of 1530 ± 5 MeV and a width of 80 ± 10 MeV. A free fit using $f_0(1500)$ instead of $f_2'(1525)$ gives a much worse log likelihood by 163. Our definition of log likelihood is such that it changes by 0.5 for a one standard deviation change in one variable, so $f_2'(1525)$ is preferred by $> 10\sigma$. A free fit including both $f_0(1500)$ and $f_2'(1525)$ gives an $f_0(1500)$ contribution only 11% of $f_2'(1525)$; for the final fit, the $f_0(1500)$ contribution is therefore fixed from that fitted to $\gamma(\pi^+\pi^-)$ discussed below, using the PDG value for the branching ratio $f_0(1500) \to K\bar{K}/f_0(1500) \to \pi\pi = 0.19$. Likewise, the small contribution from $f_2(1270) \to K\bar{K}$ is fixed from the fit to $\gamma(\pi^+\pi^-)$ using the PDG average for the branching ratio between $K\bar{K}$ and $\pi\pi$.

Close to the $\bar{K}K$ threshold, a further broad contribution from $f_0(400-1200)$ is definitely required above background. It cannot be fitted by $f_0(980) \to K\bar{K}$ because of the absence of $f_0(980)$ in $\gamma(\pi^+\pi^-)$.

The $f_0(1710) \to K^+K^-$ peaks at 1735 MeV with a width $\Gamma = 180 \pm 20$ MeV. Interference between $f_0(1710)$ and the broad $f_0(400-1200)$ can shift the mass of $f_0(1710)$ by as much as 40 MeV. An alternative fit to $f_J(1710)$ with $J^P = 2^+$ is worse by 108 in log likelihood. Remembering that three helicity amplitudes are fitted for spin 2 but only one for spin 0, the fit with $J^P = 0^+$ is preferred by $> 10\sigma$. This confirms the conclusion of Dunwoodie's analysis [14]. Fig. 17 shows contributions to the fit from individual channels and also the overall 0^+ and 2^+ contributions including interferences between channels.

The separation between spin 0 and 2 is illustrated in Fig. 18. Let us denote the polar angle of the K^+ in the K^+K^- rest frame by θ^*_{K+}, and the polar angle of the photon in the J/Ψ rest frame by θ_γ. Both distributions and the Dalitz plot are fitted simultaneously including important correlations between θ^*_{K+} and θ_γ. The upper panels show resulting fits to $\cos\theta^*_{K+}$ for $J = 0$ and 2. There is no significant difference between the two fits. The distributions should be flat for 0^+, but the interference with the tail of $f_2'(1525)$ has a large effect. The lower panels show the fits to $\cos\theta_\gamma$; the optimum fit is visibly better for $J = 0$ than $J = 2$. [If one fits only the $\cos\theta_\gamma$ distribution, it is possible to fit equally well with $J = 0$ or 2, but then the fit to $\cos\theta^*_{K+}$ gets much worse.]

We next consider $J/\Psi \to \gamma(\pi^+\pi^-)$. The $\pi\pi$ mass distribution is shown in the upper panel of Fig. 19. There is a large peak due to $f_2(1270)$ and a further small peak near 1750 MeV. There is also a small but definite shoulder which we find originates from $f_0(1500)$. The fit requires a dispersive shape for this contribution as a function of mass, hence interference with a broad contribution from $f_0(400-1200)$.

Before coming to details, we summarise the essential problems and uncertainties in fitting $\gamma(\pi\pi)$. The main problem is a substantial experimental background arising from the strong process $J/\Psi \to \rho\pi$ after loss of one photon. This background is shown in Fig. 19. Its magnitude is fixed making use of the PDG branching ratio for $J/\Psi \to \pi^+\pi^-\pi^0$, which has an error of $\pm 13\%$. However, uncertainty in the effect of a form factor on the tail of the $\rho(770)$ raises

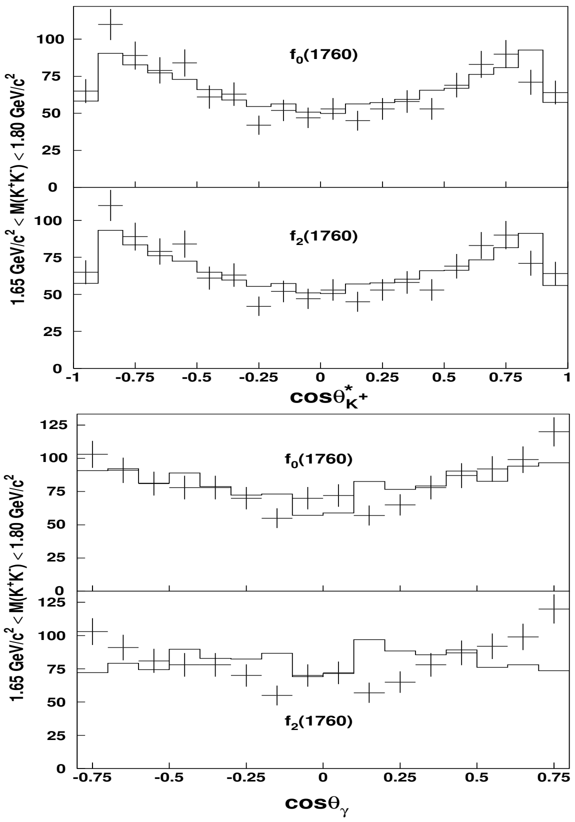

Fig. 18. Projections on to $cos\theta^*_{K^+}$ and $cos\theta_\gamma$ with 0^{++}, 2^{++} asumptions. The points are the data, and the curves are the fit results.

the overall error on the background to an estimated $\pm 18\%$. This background was also present in earlier DM2 and Mark III data [27] [18].

The uncertainty in this background is compounded by uncertainty about the precise shape of $f_0(400-1200)$. Its s-dependence has been fitted up to a mass of 1500 MeV by Zou and Bugg [33] and we adopt their parameterisation. However, its coupling constant may vary with s and there may be further s-dependence arising from the two contributions with $L = 0$ and 2. We find that the fit improves substantially if the coupling constant is given the form $\Lambda_1 + \Lambda_2 s$, where Λ_1 and Λ_2 are both complex. Alternative forms of s-dependence give fits of similar quality.

Following these general points, we return to the details of the fit to $\gamma(\pi^+\pi^-)$. The high mass contribution at ~ 1750 MeV requires spin 0. An alternative fit with spin 2 is worse in log likelihood by 18.2; a fit with both gives a dominant spin 0 component. A free fit to its mass and width gives M= 1790^{+90}_{-60} MeV, $\Gamma = 350 \pm 100$ MeV. A combined fit to present data and those for the final state $\phi\pi^+\pi^-$ [25] gives M= 1775 ± 35 MeV, $\Gamma = 220 \pm 50$ MeV. It is not well fitted by $f_0(1710)$ with PDG values of mass and width; the last panel of Fig. 19 shows this fit, which has log likelihood worse by 23.4.

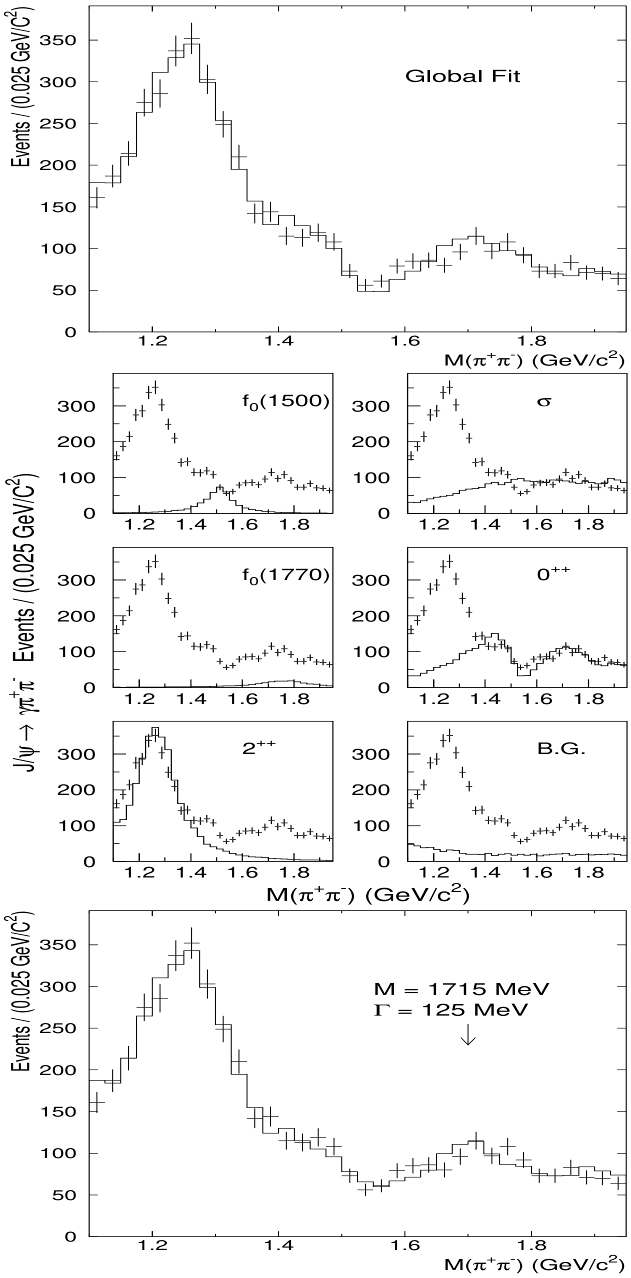

Fig. 19. The $\pi^+\pi^-$ invariant mass distribution from $J/\psi \to \gamma(\pi^+\pi^-)$. The points are the data and the full histogram in the top panel shows the maximum likelihood fit. Lower panels show individual contributions and background (B.G.) and from 0^+ and 2^+ contributions including interferences. The last panel shows a fit using PDG values of mass and width for $f_0(1710)$.

The 0^+ states in $\gamma K\bar{K}$ and $\gamma\pi\pi$ cannot be separated reliably on the basis of their masses, since interference with the broad $f_0(400-1200)$ makes it possible to shift masses over an appreciable range $\sim \pm 40$ MeV. This type of effect is well illustrated by the $f_0(1500)$, which appears as a shoulder at 1460 MeV in Fig. 19 because of such interferences.

Data on $J/\Psi \to \phi(\pi^+\pi^-)$ and $\phi(K^+K^-)$ show a definite peak in $\pi^+\pi^-$ at 1770 MeV but no significant signal in K^+K^- [25]. This is in complete contrast to our data on $J/\Psi \to \omega(\pi^+\pi^-)$ and $\omega(K^+K^-)$, where there is a strong peak at 1750 MeV in K^+K^-, but only a small, barely visible signal in $\pi^+\pi^-$ [34]. As far as we can establish, interference effects with other components are far too small to allow these vastly different branching ratios to be reconciled with a single 0^+ resonance. In fact, two 0^+ states are to be expected in the mass range 1700–1800 MeV. One is the $s\bar{s}$ state completing a nonet made of $K_0^*(1430)$, $a_0(1450)$ and $f_0(1370)$ (or $f_0(1500)$ in one scheme [35]). The second 0^+ state is a non-strange radial excitation of $f_0(1370)$. Both are likely to mix with the glueball anticipated in this mass range, so their appearance in J/Ψ radiative decays is not surprising. It is natural to associate the $f_0(1710)$ with the $s\bar{s}$ state, because of its appearance in $K\bar{K}$. The radial excitation is naturally interpreted as decaying to $\pi\pi$ and 4π. Both $\gamma\pi\pi$ and $\phi\pi\pi$ data are fitted better by $f_0(1770)$ with the parameters of Ref. [36].

We now return to the discussion of $f_2(1270)$ and $f_2'(1525)$. In earlier work by DM2 and Mark III [27] [26] [18], ratios of helicity amplitudes were determined for production of these states. They expressed their results in terms of ratios $x = h_1/h_0$ of amplitudes with helicities $h = 1$ and 0 and a ratio $y = h_2/h_0$ of helicity 2 to 0. The relation between the magnitudes $C_1,\ C_2,\ C_3$ used in our fit and x, y is as follows:

$$x = \frac{\frac{E_{f_2}}{M_{f_2}} + \frac{2|\vec{q}|^2}{M_{f_2}} B_2(Q_{\psi\gamma f_2}) \frac{C_3}{C_1}}{\sqrt{\frac{1}{3}} + \sqrt{\frac{4}{3}} \frac{|\vec{q}|^2}{M_{f_2}^2} B_2(Q_{\psi\gamma f_2}) \frac{C_2}{C_1}} \tag{6}$$

$$y = \frac{1}{\sqrt{\frac{1}{6}} + \sqrt{\frac{2}{3}} \frac{|\vec{q}|^2}{M_{f_2}^2} B_2(Q_{\psi\gamma f_2}) \frac{C_2}{C_1}} \tag{7}$$

Here, $\vec{q}$ is the momentum of photon; E_{f_2}, M_{f_2} are the energy and mass of vector meson respectively. $B_2(Q_{\psi\gamma f_2})$ is the Blatt-Weisskopf barrier factor, and $B_2(Q_{xyz}) = 1/\sqrt{Q_{xyz}^4 + 3Q_{xyz}^2 Q^0 + 9Q_0^4}$, $Q_0^2 = \frac{0.22}{3}$, $Q_{xyz}^2 = \frac{(s_x+s_y-s_z)^2}{4s_x} - s_y, s_x = E_x^2 - P_x^2$.

Our results for these ratios differ significantly from the earlier work. For $f_2(1270)$ we find $x = 0.66 \pm 0.14$, $y = 0.46 \pm 0.20$, compared with Mark III results $x = 0.96 \pm 0.07$, $y = 0.06 \pm 0.08$ and DM2 results $x = 0.83 \pm 0.06$, $y = 0.01 \pm 0.06$. For $f_2'(1525)$ we find $x = 1.58 \pm 0.12$, $y = 1.07 \pm 0.23$, compared with Mark III and DM2 results $x = 0.65 \pm 0.09$, $y = -0.03 \pm 0.11$; $x = 1.08 \pm 0.10$, $y = 0.19 \pm 0.11$. These are definite differences, since the corresponding angular distributions in terms of $\cos\theta_{\pi,K}$ and $\cos\theta_\gamma$ differ significantly from the earlier results, possibly because of differences in acceptance and selection procedures. Fig. 20 shows fits to these angular distributions from present data; dot-dashed and dashed curves show earlier results of DM2 and Mark III respectively. In our present fit, we allow some 0^+ contribution under the f_2 peaks, while previous analyses ignored the small 0^+ contributions. Our values lie closer to values for an E1 transition, $x = \sqrt{3}$, $y = \sqrt{6}$, and close to Kramer's prediction [37].

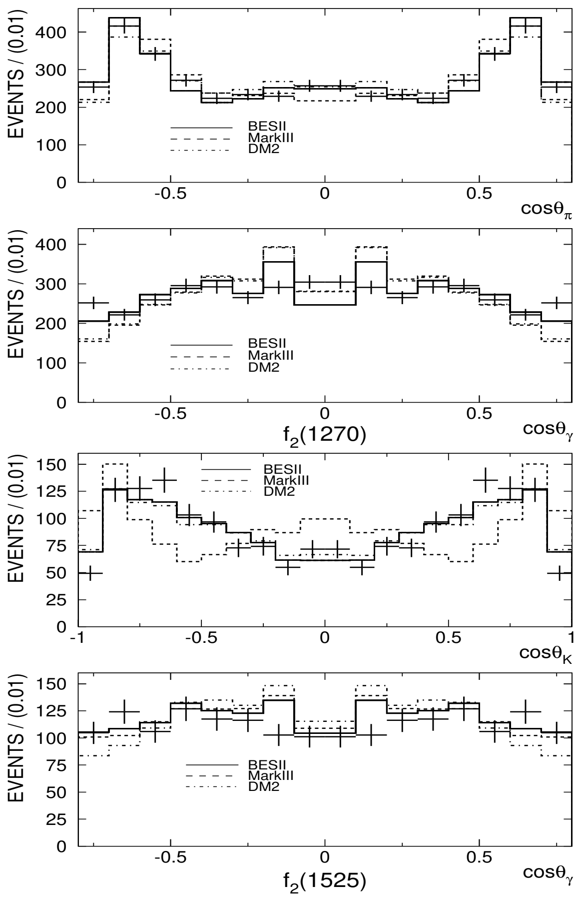

Fig. 20. Symmetrized projections on to $cos\theta^*_{K^+}$, $cos\theta_\gamma$ of $f_2(1270)$ and $f_2'(1525)$ with different x, y values obtained by BES II, Mark III and DM2 respectively.

As metioned in the part on data selection, we use $\mathrm{M}^2(\gamma\pi^\pm) > 1.1$ GeV^2 on the Dalitz plot to reject the $\rho^\pm\pi^\mp$ background events. After such a cut, the polar angle of pion in the $\pi\pi$ system is limited in: $\sim |cos\theta_\pi| < 0.8$. One question is whether the resolution based on the present data sample can describe the whole angular range. To answer it, two tests are performed. First, we increase the data sample a little at the edges of $cos\theta_\pi$ by using $\mathrm{M}(\gamma\pi^\pm) < 50$ MeV. If we take the previous best resolution to describe it, the angular distributions ($m_{\pi^+\pi^-} \in (1.10, 1.40)$ GeV) are shown in Fig. 21 (a) and (b). It shows that the resolution can fit the edge part of $cos\theta_\pi$ as well. Secondly, we remove the cut $\mathrm{M}^2(\gamma\pi^\pm) > 1.1$ GeV^2 and then analyze the $\gamma\pi^+\pi$ data sample (11911 events where 4041 (33.9%) are from $\rho\pi$ background). There we just use the background estimate method described previously. Fig. 21 (c) and (d) show the angular distribution from the fit. Fig. 21 d) descibes the $cos\theta_\pi$ well, but Fig. 21 c) doesn't; it gives a poor description of the $cos\theta_\gamma$ distribution. This may be because the $\rho\pi$ generator can't describe expermental data precisely. So for the data sample, the fewer background events the better for our partial wave analysis. Eventually we include the results from these two tests in assessing the errors of the branching ratios and helicity parameters x, y.

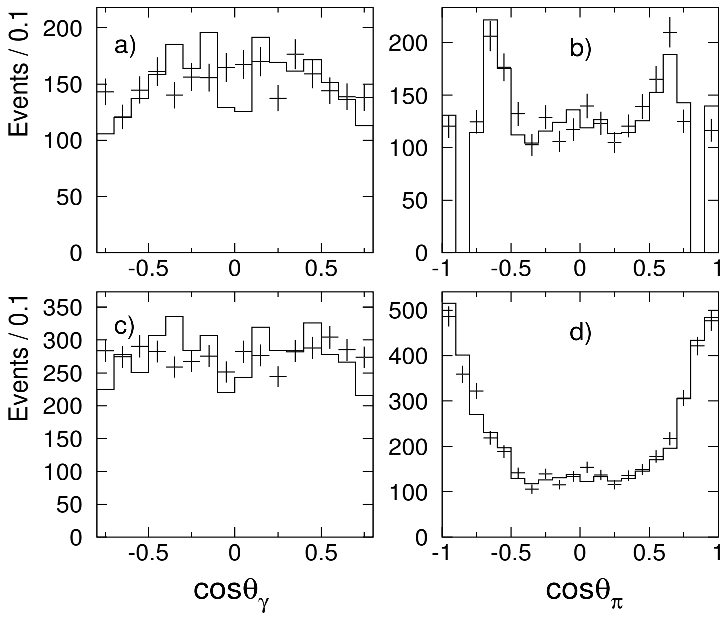

Fig. 21. Angle distributions from two tests which based on different data samples.

We now discuss branching ratios, which are summarised in Tab. 3. The detection efficiencies of the individual resonances used to calculate the banching ratios are obtained as follows. The partial wave fit provides the magnitudes and phases of the different partial amplitudes as well as the interference terms. We use the intensity from these amplitudes to weight both the complete set of generated Monte Carlo events and the set which survives the selection procedure. The ratio between these two weighted sets is just the efficiency we need. This table also summarises changes in log likelihood when each channel is removed from the fit and all others are re-optimised.

Branching ratios for production and decay of $f_2'(1525)$ and $f_0(1710)$ to all charge states are somewhat below PDG averages. The same discrepancy has been observed in several other channels, and it appears that BES determinations of branching ratios are systematically $\sim 25\%$ lower than those originating from Mark III and DM2. This discrepancy probably arises from systematic uncertainties in luminosities, which have an error of order 10% for each experiment. From the 1734 events attributed to $f_0(1710) \to K^+K^-$, allowing a factor 2 for $K^0\bar{K}^0$ final states, we find

$$BR[J/\Psi \to \gamma f_0(1710),\ f_0(1710) \to K\bar{K}] = (6.7 \pm 1.1) \times 10^{-4}. \quad (8)$$

This compares with the PDG average $(8.5^{+1.2}_{-0.9}) \times 10^{-4}$. Some of the discrepancy can be attributed directly to constructive interference fitted to present data between $f_0(1710)$ and the broad component due to $f_0(400-1200)$. This interference is absent from the work of Mark III and DM2. If we omit it, the value of equn. (8) rises to $(8.4 \pm 1.3) \times 10^{-4}$.

Channel	Branching fraction ($\times 10^4$)	Events	ΔS
$J/\Psi \to \gamma f_2'(1525),\ f_2'(1525) \to K^+K^-$	1.24 ± 0.20	771	> 100
$J/\Psi \to \gamma f_0(1710),\ f_0(1710) \to K^+K^-$	3.36 ± 0.54	1734	> 100
$J/\Psi \to \gamma f_2(1270),\ f_2(1270) \to \pi^+\pi^-$	7.96 ± 0.96	3232	> 100
$J/\Psi \to \gamma f_0(1500),\ f_0(1500) \to \pi^+\pi^-$	1.01	483	30.2
$J/\Psi \to \gamma f_0(1770),\ f_0(1770) \to \pi^+\pi^-$	0.52 ± 0.19	208	22.1
$J/\Psi \to \gamma f_0(400-1200) \to \gamma\pi^+\pi^-$	23.9 ± 12.4	2431	> 100

Table 3
Branching fractions for each channel after correction for background; changes in $S = -\log$ likelihood due to each contribution. The branching fraction for $f_0(1500) \to \pi^+\pi^-$ is discussed in the text.

For $f_0(1770)$ we find, for all charge states:

$$BR[J/\Psi \to \gamma f_0(1770),\ f_0(1770) \to 2\pi] = (0.78 \pm 0.27) \times 10^{-4}. \tag{9}$$

The large error arises from correlations between magnitudes fitted to $f_0(1770)$ and $f_0(1500)$, whose contribution is discussed below. From Mark III data on radiative decays to $\pi^+\pi^-\pi^+\pi^-$, Bugg *et al.* [12] find a 0^+ signal at 1750 ± 15 MeV with $\Gamma = 160 \pm 40$ MeV; with somewhat lower statistics, BES data [13] give M$= 1740^{+30}_{-25}$ MeV. It is plausible to associate this large 4π signal with the non-strange $f_0(1770)$. The derivation of the 4π branching ratio requires careful account of the interferences within the 4π final states; they are different for different charge combinations, since the $f_0(400-1200)$ which dominates the decay appears only in $\pi^+\pi^-$ and $\pi^0\pi^0$. Chen *et al.* [38] have evaluated these interferences; the resulting branching ratio for all 4π charge states is

$$BR[J/\Psi \to \gamma f_0(1770), f_0(1770) \to 4\pi] = (8.1 \pm 1.1) \times 10^{-4}. \tag{10}$$

From equns. (9) and (10),

$$\frac{BR[f_0(1770) \to 2\pi]}{BR[f_0(1770) \to 4\pi]} = (9.6 \pm 3.6) \times 10^{-2}. \tag{11}$$

In view of the 25% systematic discrepancy observed between BES and Mark III + DM2, this should probably be increased to $(12 \pm 5)\%$. The 4π decays dominate strongly, again pointing to non-strange character of $f_0(1770)$.

We consider next the contribution of $f_0(1500)$. In the 2π mass spectrum of Fig. 19, there is a slight but definite shoulder due to $f_0(1500)$; the mass scan gives an optimum mass 1510^{+10}_{-15} MeV. Omitting it from the final fit, log likelihood gets worse by 30.2. However, its magnitude is not well determined because of (i) interference with $f_0(400-1200)$, (ii) uncertainty in the s-dependence of $f_0(400-1200)$, (iii) the difficulty of separating the experimental background from $f_0(400-1200)$.

From Refs. [13, 38] the value $BR[J/\Psi \to \gamma f_0(1500), f_0(1500) \to 4\pi] = (4.8 \pm 0.8) \times 10^{-4}$. Next, Thoma [39] has determined the ratio $BR[f_0(1500) \to 4\pi]/BR[f_0(1500) \to 2\pi] \sim 1.55$, using Crystal Barrel data at rest. The PDG quotes a ratio 3.4 ± 0.8 [23]; however, that value was obtained ignoring interferences within the 4π channel. When these are evaluated as in Ref. [38], the corrected value is (2.04 ± 0.56), consistent with Thoma's determination. Then the predicted branching ratio is

$$BR[J/\Psi \to \gamma f_0(1500), f_0(1500) \to 2\pi] = (2.1 \pm 1.0) \times 10^{-4}. \tag{12}$$

The large error arises from adding in quadrature errors for (i) the 4π branching ratio in Refs. [16, 17], (ii) the error of Thoma's determination, (iii) the luminosity ratio between present data and Mark III. The final fit to present data gives a value for equn. (12) of 1.5×10^{-4}. The discrepancy could arise from the 25% systematic discrepancy in all branching ratios between BES and results of Mark III + DM2.

Both data sets require some contribution from $f_0(400-1200)$. Neither is well determined because of the uncertainty in possible s-dependence of its coupling constant. A rough estimate of the relative decays to $K\bar{K}$ and $\pi\pi$ may be obtained:

$$f_0(400-1200) \to K\bar{K}/f_0(400-1200) \to \pi\pi = 0.18 \pm 0.11 \tag{13}$$

From present data, the relative branching ratio $\gamma f_2(1270)/\gamma f_2'(1525) = 4.9 \pm 1.4$. The large error arises from uncertainties in interferences with other components in the fit, particularly $f_0(1500)$ and $f_0(400-1200)$. From PDG averages, one finds 2.8 ± 0.5. However, in the earlier work used by the PDG, interferences with $f_0(1500)$ and $f_0(400-1200)$ were not considered. From the coupling of two gluons to $(u\bar{u} + d\bar{d})$ and $s\bar{s}$, one expects a ratio 2 for ideal mixing in the 2^+ nonet. However, this value will be increased by phase space factors q for an E1 transition, and q^5 for E3, where q is the momentum of the photon. Form factors are expected to be small because the $c\bar{c}$ annihilation is pointlike. The predicted ratio becomes 2.19 for an E1 transition and 3.17 for E3. The observed ratio is somewhat higher. However, if the s-dependence of the $f_0(400-1000)$ contribution is restricted to be the same for $\pi\pi$ and $K\bar{K}$, the ratio falls to 3.5 ± 0.9, consistent with prediction within the error.

Finally, we remark that we have tried adding contributions from $f_0(1370)$ to the fits to both $\pi\pi$ and $K\bar{K}$ final states. The contributions are not statistically significant. This is not surprising, since it is known [40] that $f_0(1370)$ decays dominantly to 4π.

In summary, the mass and width observed for $f_0(1710)$ in $\gamma(K^+K^-)$ data are slightly above PDG values. The data confirm Dunwoodie's conclusion that $J^P = 0^+$. The analysis of early BES data on $J/\Psi \to \gamma(K\bar{K})$ [41] reached the conclusion that separate resonances are required at 1696 MeV and 1781 MeV. That work used an analysis in terms of moments. Such analysis suffers from the problem of incomplete acceptance near the beam direction. It favoured $J^P = 2^+$ for the lower resonance and 0^+ for the upper one. The present analysis fits much higher statistics directly using the maximum likelihood method, which takes into account fully the angular acceptance. The conclusion is again that separate resonance are required in $\pi\pi$ and $K\bar{K}$, but it is now clear that both have $J^P = 0^+$.

From present $\gamma(\pi\pi)$ data and earlier data on $J/\Psi \to \gamma(4\pi)$, we find $f_0(1770) \to \pi\pi/f_0(1770) \to 4\pi = (9.6 \pm 3.6)\%$. The strong decay to 4π is consistent with a radial excitation of a non-strange meson, while the observed decay of $f_0(1710)$ to $K\bar{K}$ suggests an $s\bar{s}$ state. Their appearance in J/Ψ radiative decays suggests mixing with the 0^+ glueball predicted near this mass range. The $\gamma(\pi\pi)$ data require the presence of $f_0(1500) \to \pi\pi$, with a branching ratio which is at the bottom of the error band predicted from its observation in $J/\Psi \to \gamma(4\pi)$.

References

[1] S. J. Brodsky, T. A. DeGrand, R. R. Horgan and D. G. Coyne, Phys. Lett. B73 (1978) 203; K. Koller and T. Walsh, Nucl. Phys. B140 (1978) 449.

[2] A. Billoire *et al.*, Phys. Lett. B80 (1979) 381;
R. Lacaze and H. Navelet, Nucl. Phys. B186 (1981) 247.

[3] G. Bali, K. Schilling, A. Hulsebos, A. Irving, C. Michael, and P. Stephenson, Phys. Rev. B309 (1993) 378.

[4] C. Michael, Proceedings of Hadron 97, AIP Conf. Series 432 (1997) 657.

[5] W. Lee, and D. Weingarten, hep-lat/9805029.

[6] C. Morningstar, and M. Peardon, Phys. ReV D60 (1999) 034509.

[7] A. Anisovich, *et al.*, Phys. Lett B323 (1994) 233.

[8] A. Bertin, *et al.*, Phys. Rev. D57 (1998) 55.

[9] F. Antinori, *et al.*, Phys. Lett. B353 (1995) 589.

[10] D. Barberis, *et al.*, Phys. Lett. B413 (1997) 217.

[11] M. Reyes *et al.*, Phys. Rev. Lett. 81 (1998) 4079.

[12] D. Bugg *et al.*, Phys. Lett. B353 (1995) 378.

[13] J. Bai, *et al.*, Phys. Lett. B472 (2000) 207.

[14] W. Dunwoodie, Proceedings of Hadron 97, AIP Conf. Series 432 (1997)

[15] J. Sexton *et al.*, Phys. Rev. Lett. 75 (1995) 4563.

[16] C. Edwards *et al.*, Phys. Rev. Lett. 48 (1982) 458.

[17] Ph. Gavillet *et al.*, Zeit. Phys. C16 (1982) 119;
D. Aston *et al.*, Nucl. Phys. B301 (1988) 525.

[18] R. M. Baltrusaitis *et al.*, Phys. Rev. D35 (1987) 2077.

[19] T. A. Armstrong *et al.*, Phys. Lett. B227 (1989) 186.

[20] D. Barberis *et al.*, Phys. Lett. B453 (1999) 305.

[21] D. Barberis *et al.*, Phys. Lett. B453 (1999) 316.

[22] B. French *et al.*, Phys. Lett. B460 (1999) 213.

[23] Particle Data Group (PDG), Euro . Phys. Journ. C15 (2000) 1.

[24] D. Bugg *et al.*, Phys. Lett. B486 (2000) 49.

[25] *Study of* $J/\Psi \to \phi(K^+K^-)$ *and* $\phi(\pi^+\pi^-)$, BES Collaboration, to be submitted to ?? Physics Letters B.

[26] J.E. Augustin *et al.*, Phys. Rev. Lett. 60 (1988) 2238.

[27] J.E. Augustin *et al.*, Zeit. Phys. C36 (1987) 369.

[28] W. Braunschweig *et al.*, Phys. Lett. B63 (1975) 115.

[29] T. Himel *et al.*, Phys. Lett. 45 (1980) 1146.

[30] J. Bai *et al.*, Phys. Rev. Lett. 76 (1996) 3502.

[31] T. Bolton, "Radiative Decays of the J/Ψ to two Pseudoscalar Final States", Ph. D thesis.

[32] Z. Guo, Ph.D. thesis, IHEP, Beijing (2000).

[33] B.S. Zou and D.V. Bugg, Phys. Rev. D48 (1993) 3948.

[34] *Data on* $J/\Psi \to \omega(K^+K^-)$ *and* $\omega(\pi^+\pi^-)$, BES Collaboration, to be submitted to ?? Physics Letters B.

[35] A.V. Anisovich *et al.*, Phys. Lett. B467 (1999) 289 and papers referenced there.

[36] A. Anisovich *et al.*, Phys. Lett. B449 (1999) 154.

[37] M. Kramer, Phys. Lett. B74 (1978) 361.

[38] J. Chen, X-Q. Li and B.S. Zou, Phys. Rev. D62 (2000) 034011.

[39] U. Thoma *Hadron '99*, Nucl. Phys. A675 (2000) 7bc.

[40] Resonances in $\bar{p}p \to \eta\pi^+\pi^-\pi^+\pi^-$ at rest, A.V. Anisovich *et al.*, Nucl. Phys. A. (in press)

[41] J.Z. Bai *et al.*, Phys. Rev. Lett. 77 (1996) 3959.